ceding paper in this issue.
(3) D. C. Klein, J. L. Weller, A. Parfitt, and K. L. Kirk in "Chemical Tools in Catecholamine Research", Vol. II, O. Almgren, S. Carlsson, and J. Engel, Eds., North-Holland Publishing Co., Amsterdam, 1975, pp 293–300; other manuscripts submitted or in preparation.
(4) Although there exists only limited evidence for Brønsted relationships between the p*K*s of carbon acids and their "kinetic acidities", we assume rates of exchange to reflect the order of acidities of imidazole ring hydrogens, and use the concepts interchangeably. Cf. J. R. Jones, "The Ionization of Carbon Acids", Academic Press New York, N.Y., 1973, Chapter 8.
(5) Unpublished data. See also; H. Matsuo, M. Ohe, F. Sakiyama, and K. Narita, *J. Biochem. (Japan)*, **72**, 1057 (1972); J. H. Bradbury, B. E. Chapman, and F. A. Pellegrino, *J. Am. Chem. Soc.*, **95**, 6139 (1973).
(6) K. L. Kirk and L. A. Cohen *ACS Symp. Ser.* **No. 28**, Chapter 2 (1976).
(7) Exchange data for some nitroimidazoles in D_2O (100 °C) have been reported: H. A. Staab, H. Irngartinger, A. Mannschreck, and M.-Th. Wu, *Justus Liebgis Ann. Chem.*, **695**, 55 (1966).
(8) NMR δ values for the imidazole ring hydrogens depend almost entirely on the σ^R values of substituents (manuscript in preparation); e.g., for X = NO_2 or CO_2R (series **1** or **2**), H-4 and H-5 appear at lower field than H-2, while the order is reversed for X = F or CH_3.
(9) J. Elguero, E. Gonzalez, and R. Jacquier, *Bull. Soc. Chim. Fr.*, 2998 (1967).
(10) J. C. Reepmeyer, K. L. Kirk, and L. A. Cohen, *Tetrahedron Lett.*, 4107 (1975).
(11) L. A. Cohen and S. Takahashi, *J. Am. Chem. Soc.*, **95**, 443 (1973).
(12) Compound **2a** is 2.7 units more basic than **1a**; this large difference has been attributed to the fact that a positive charge on N-3 is more readily tolerated when the nitro group is more distant (on C-5): A. Grimison, J. H. Ridd, and B. V. Smith, *J. Chem. Soc.*, 1352 (1960).
(13) K. L. Kirk, W. Nagai, and L. A. Cohen, *J. Am. Chem. Soc.*, **95**, 8389 (1973).
(14) The instability of 1-alkyl-5-aminoimidazoles has been noted previously: see, e.g., A. H. Cook, J. D. Downer, and I. Heilbron, *J. Chem. Soc.*, 2028 (1948); G. Shaw, R. N. Warrener, D. N. Butler, and R. K. Ralph, *ibid.*, 1625 (1952). Somewhat greater stability is observed for 1-alkyl-4-aminoimidazoles [R. Buchman, P. F. Heinstein, and J. N. Wells, *J. Med. Chem.*, **17**, 1168 (1974)] and for 4-alkyl-5-aminoimidazoles [unpublished observations].
(15) Theoretical calculations suggest **8** to be more stable than **9** by ~0.5 kcal/mol: N. Boder, M. J. S. Dewar, and A. J. Harget, *J. Am. Chem. Soc.*, **92** 2929 (1970).
(16) C. R. Ganellin in "Molecular and Quantum Pharmacology", E. Bergmann and B. Pullman, Eds., D. Reidel Publishing Co., Dordrecht, Holland, 1974, pp 43–53.
(17) According to the data of ref 7, exchange of **4a** in D_2O (100 °C) occurs at both H-5 and H-2 in the ratio 3:5. We were unable to achieve detectable solubility of **4a** in D_2O, even at 100 °C; in D_2O–Me_2SO-d_6 (4:1), 10% loss of the H-2 signal was observed in 13.5 h at 100 °C, but there was no detectable loss of the H-5 signal. According to the same report, total exchange of H-2 and H-5 occurs in 0.8 N NaOD (100 °C) in 12 h; our results agree with respect to H-5, but we found no measurable exchange of H-2 under the same conditions.
(18) Although the data for 2-fluorohistidine are gratifyingly consistent with intramolecular participation by the α-amino group, the evidence is not yet unequivocal; accordingly, exchange studies with α-*N*-acyl-2-fluorohistidines are in progress.
(19) In tautomer **10**, C-4 should be somewhat lower in electron density than in the true imidazole structure; accordingly, **10** may be stabilized by hyperconjugation or electron release from the group attached to C-4. An investigation of this possibility is in progress.
(20) C. B. Klee, K. L. Kirk, and L. A. Cohen, unpublished experiments.
(21) M. Eigen, *Angew. Chem., Int. Ed. Engl.*, **3**, 1 (1964).
(22) J. Stuehr, E. Yeager, T. Sachs, and F. Hovorka, *J. Chem. Phys.*, **38**, 587 (1963).
(23) J. A. Elvidge, R. R. Jones, C. O'Brien, E. A. Evans, and H. C. Sheppard, *Adv. Heterocycl. Chem.*, **16**, 1 (1974).
(24) (a) D. A. Shirley and P. W. Alley, *J. Am. Chem. Soc.*, **79**, 4922 (1957); (b) K. L. Kirk, *J. Org. Chem.*, in press (1978).
(25) J. A. Zoltewicz, G. Grahe, and C. L. Smith, *J. Am. Chem. Soc.*, **91**, 5501 (1969).
(26) P. Luger, G. Kothe, and H. Paulsen, *Chem. Ber.*, **107**, 2626 (1974); I-Nan Hsu and B. M. Craven, *Acta Crystallogr., Sect. B*, **30**, 988 (1974); S. Martinez-Carrera, *ibid.*, **20**, 783 (1966).
(27) J. B. Stothers, "Carbon-13 NMR Spectra", Academic Press, New York, N.Y., 1972, Chapters 9, 10.
(28) R. Hoffmann, *Acc. Chem. Res.*, **4**, 1 (1971); W. Adam, A. Grimison, and R. Hoffmann, *J. Am. Chem. Soc.*, **91**, 2590 (1969).
(29) All commercial and synthesized compounds were checked for purity and identity by TLC, NMR, and mass spectroscopy.
(30) W. E. Allsebrook, J. M. Gulland, and F. L. Story, *J. Chem. Soc.*, 232 (1942).
(31) G. G. Gallo, C. R. Pasqualucci, P. Radaelli, and G. C. Lancini, *J. Org. Chem.*, **29**, 862 (1964).
(32) E. Regel and K.-H. Buchel, *Justus Liebigs Ann. Chem.*, 145 (1977).
(33) K. L. Kirk and L. A. Cohen, *J. Am. Chem. Soc.*, **95**, 4619 (1973).
(34) I. E. Balaban, *J. Chem. Soc.*, 268 (1930).
(35) J. J. Baldwin, P. A. Kasinger, F. C. Novello, J. M. Sprague, and D. E. Duggan, *J. Med. Chem.*, **18**, 895 (1975). We are indebted to Dr. Baldwin for supplying a generous sample of this compound.
(36) A. G. Beaman, W. Tantz, T. Gabriel, and R. Duschinsky, *J. Am. Chem. Soc.*, **87**, 389 (1965).
(37) G. Lancini and E. Lazzari, *J. Heterocycl. Chem.*, **3**, 152 (1966).
(38) Comparable temperature effects (up to 50 °C) have been reported: A. C. M. Paiva, L. Juliano, and P. Buschcov, *J. Am. Chem. Soc.*, **98**, 7645 (1976); S. P. Datta and A. K. Grzybowski, *J. Chem. Soc. B*, 136 (1966).
(39) A. K. Covington, R. A. Robinson, and R. G. Bates, *J. Phys. Chem.*, **70**, 3820 (1966).

Spiro Meisenheimer Complexes from 7-(2-Hydroxyethoxy)-4-nitrobenzofurazan and 7-(2-Hydroxyethoxy)-4-nitrobenzofuroxan. A Kinetic Study in Aqueous Solution

Guy Ah-Kow,[1a] Francois Terrier,*[1a,b] and Florence Lessard[1a]

Laboratoire de Physicochimie des Solutions, E.N.S.C.P., 75231 Paris, Cédex 05, France, and Département de Chimie, Faculté des Sciences de Rouen, 76130 Mont Saint Aignan, France

Received February 21, 1978

Cyclization of 7-(2-hydroxyethoxy)-4-nitrobenzofurazan (**3**) and 7-(2-hydroxyethoxy)-4-nitrobenzofurazan (**6**) occurs in aqueous solution containing base to give the spiro Meisenheimer-type complexes **5** and **8**, which have a high thermodynamic stability. A similar reaction occurs in Me_2SO where the structures of **5** and **8** could be fully characterized by ^1H NMR spectroscopy. The kinetics of formation and decomposition of **5** and **8** have been studied by the stopped-flow method between pH 1 and 12 in aqueous solution. It is found that **5** is only 2.5-fold more stable than **8** ($pK_a^5 = 6.86$; $pK_a^8 = 7.26$), but it forms and decomposes much faster than its furoxanic analogue. These differences in rates are attributed to the *N*-oxide group, which probably exerts a very unfavorable influence on the C–O bond-forming and bond-breaking processes associated with formation and decomposition of the furoxanic adduct **8**. The ring opening of **5** and **8** is subject to general acid catalysis in aqueous solution with a Brønsted coefficient α of 0.44. The results are discussed by comparison with those obtained for benzenic analogues.

The proposal[2–4] that the antileukemic activity of some benzofurazan and benzofuroxan derivatives may be due to their ability to easily form Meisenheimer-type complexes with essential cellular SH and/or amino groups has increased interest in the adducts obtained from covalent addition of nucleophiles to these compounds. There is now convincing structural evidence, mainly from NMR studies, that such adducts are formed in the reaction of a variety of mono- and dinitrobenzofurazans and -benzofuroxans with hydroxide and methoxide ions.[5–10] The thermodynamic and kinetic data for

0022-3263/78/1943-3578$01.00/0

the formation and decomposition of this class of adducts have been reported mainly for the dinitro complexes **1** and **2**.[2a,9,11] This is because formation of the mononitro adducts is frequently complicated by the occurrence of a number of other reactions, some of which are irreversible.[8b,10] In order to avoid these complications and to carry out a comprehensive quantitative analysis of the formation and decomposition of mononitro adducts, we became interested in furazanic and furoxanic substrates leading to the formation of spiro complexes. Such systems have been successfully used in benzenic series.[12-14] In the present work, we report data obtained for the formation and decomposition of spiro complexes **5** and **8** derived from the cyclization of 7-(2-hydroxethoxy)-4-nitrobenzofurazan (**3**) and 7-(2-hydroxyethoxy)-4-nitrobenzofuroxan (**6**), respectively, in aqueous solution.

Results

When base is added to an aqueous solution of the yellow-colored parent ethers **3** and **6**, there is an immediate appearance of colorless species with absorption spectra showing maxima at 330 and 339 nm, respectively. Similar spectra are obtained in Me_2SO solution, showing that the same species form in both solvents. Since ^1H NMR measurements in water were precluded by low solubility of the substrates, confirmation that these species are the spiro complexes **5** and **8** was

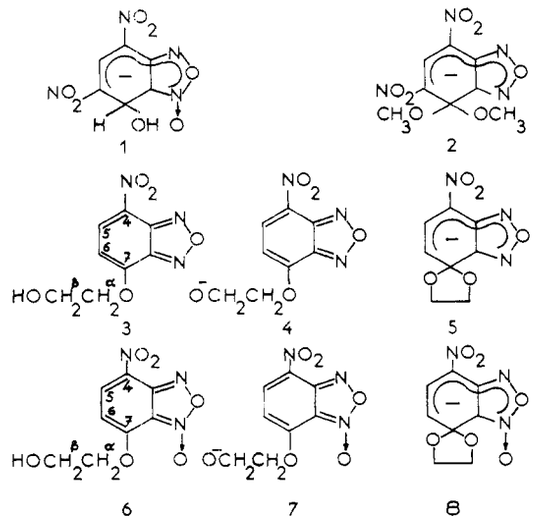

obtained from ^1H NMR spectroscopy in Me_2SO solution. Thus, addition of base to a solution of **3** or **6** in Me_2SO-d_6 results in an immediate reduction in the intensity of the signals characteristic of the ring and methylenic protons of **3** (δ, internal reference Me_4Si, 8.48 (H-5, d, J = 10 Hz), 8.02 (H-6, d, J = 10 Hz), 4.64 (α-CH_2, t), 3.84 (β-CH_2, t)) and **6** (δ 8.58 (H-5, d, J = 9 Hz), 6.83 (H-6, d, J = 9 Hz), 4.33 (α-CH_2, t), 3.83 (β-CH_2, t)) and the development of new sets of signals consistent with the postulated structures of **5** and **8**. In particular, as expected on formation of anionic complexes, the ring protons H-5, H-6 now absorb at higher field and give two doublets which are seen at δ 6.84 and 6.25 (J = 10 Hz) in the case of **5** and δ 7.12 and 4.95 (J = 9 Hz) in the case of **8**. Also, in conformity with results reported for benzenic unsymmetrical spiro adducts,[14] the nonequivalent dioxolane methylene protons of **5** and **8** give rise to a complex multiplet centered at 4.16 ppm in both cases. The resolution of these multiplets was not sufficient to allow an AA′ BB′ analysis. After the addition of 1 equiv of base was completed, the stable spectra consisted only of the signals associated with **5** and **8**. They were also similar to the spectra of solutions in Me_2SO-d_6 of the complexes **5** and **8** isolated as crystalline potassium salts (see Experimental Section).

The formation of **5** and **8** is essentially complete at pH 10.

Scheme I

$$\underset{\text{(GOH)}}{\mathbf{3}\ (\text{or } \mathbf{6})} \underset{k_{-1}}{\overset{k_1}{\rightleftharpoons}} \underset{\text{spiro complex}}{\mathbf{5}\ (\text{or } \mathbf{8})} + H^+ \qquad (1)$$

$$\underset{\text{(GOH)}}{\mathbf{3}\ (\text{or } \mathbf{6})} + OH^- \overset{K}{\rightleftharpoons} \underset{\text{(GO}^-\text{)}}{\mathbf{4}\ (\text{or } \mathbf{7})} \underset{k_{-2}}{\overset{k_2}{\rightleftharpoons}} \underset{\text{spiro complex}}{\mathbf{5}\ (\text{or } \mathbf{8})} \qquad (2)$$

To carry out a comprehensive thermodynamic and kinetic study of the formation and decomposition of these spiro adducts, we have investigated the reactions in the pH range of 1–12, using dilute hydrochloric acid solutions, various buffer solutions, and dilute potassium hydroxide solutions. The ionic strength was always kept constant at 0.2 M by adding KCl as needed. All pH values have been measured relative to the standard state in pure water, allowing the calculation of the hydrogen ion concentration $[H^+]$ of the solutions from the hydrogen ion activity a_{H^+} by means of the relation $[H^+] = a_{H^+}/\gamma_\pm$, where $\gamma_\pm$ is the trace activity coefficient in 0.2 M KCl ($\gamma_\pm = 0.75$[15]).

Equilibrium Measurements. In the large pH range studied, the possible pathways for interconversion of the glycol ethers **3** and **6** (GOH) and corresponding adducts **5** and **8** are shown in Scheme I. Whereas the first pathway involves direct internal cyclization of GOH, the second pathway, which is evidently much more favored in alkaline media, involves a rapid proton transfer from the glycol side chain to base followed by a slower internal cyclization of the formed glycolate anions (GO^-) **4** and **7**.

As previously pointed out by different workers,[12c,d13] the values of the equilibrium constant K governing the ionization of the OH group of the parent glycols are unlikely to be much higher than 0.1 M^{-1} in water. Hence, at the pH used in the present work, the product $K[OH^-]$ will be $\ll 1$, and the anion concentration $[GO^-]$ can be neglected compared to the glycol concentration [GOH]. Accordingly, the stoichiometric equilibrium constant K_c (eq 3) usually associated to the conversion of GOH to spiro adducts through eq 2 may be reduced to the simplified eq 4 from which eq 5 can be deduced. In eq 5 K_2 is the equilibrium constant governing the internal cyclization of GO^-. Furthermore, relation 7 holds between K_c and the equilibrium constant K_a (eq 6) associated with the formation of adducts through eq 1 at μ = 0.2 M (K_w is the autoprotolysis constant of water; pK_w = 14.17 at 20 °C).

$$K_c = \frac{[\text{complex}]}{([\text{GOH}] + [\text{GO}^-])[\text{OH}^-]} \qquad (3)$$

$$K_c = \frac{[\text{complex}]}{[\text{GOH}][\text{OH}^-]} \qquad (4)$$

$$K_c = KK_2 \qquad (5)$$

$$K_a = \frac{[\text{complex}][\text{H}^+]}{[\text{GOH}]} \qquad (6)$$

$$K_a = K_c \times \frac{K_w}{\gamma_\pm^2} \qquad (7)$$

Measurements of the equilibrium optical densities at the absorption maxima of the adducts were made at 20 °C in buffered solutions in the pH ranges 6.5–8 and 6.8–8.5 for **5** and **8**, respectively. As expected, a plot, not shown, of log $(OD - OD_0)/(OD_c - OD)$ vs. pH according to the equation

$$\log \frac{OD - OD_0}{OD_c - OD} = \log Ka + pH + \log \gamma_\pm \qquad (8)$$

where OD is the equilibrium optical density at a given pH, OD_c the optical density in a basic solution where complex formation is quantitative and OD_0 the optical density of the parent

Table I. Experimental and Calculated Pseudo-First-Order Rate Constants, k_{obsd}, k_f, and k_d, for the Formation and Decomposition of the Furazanic Adduct 5 in Water[a]

pH	k_{obsd}, s^{-1}	k_f, s^{-1}	k_d, s^{-1}	pH	k_{obsd}, s^{-1}	k_f, s^{-1}	k_d, s^{-1}
1.30[b]	147	3.1×10^{-4}	147	5.29[c]	0.24	4.80×10^{-3}	0.235
1.46[b]	118	3.56×10^{-4}	118	5.98[d]	0.23	2.08×10^{-2}	0.208
1.72[b]	63.4	3.49×10^{-4}	63.4	6.30[d]	0.275	4.7×10^{-2}	0.227
1.98[b]	36	3.6×10^{-4}	36	6.72[d]	0.386	0.137	0.249
2.04[b]	30.5	3.5×10^{-4}	30.5	7.05[d]	0.605	0.327	0.278
2.12[b]	24.3	3.28×10^{-4}	24.3	7.38[d]	0.915	0.656	0.26
2.20[b]	18.8	3.12×10^{-4}	18.8	7.52[e]	1.34	1.045	0.294
2.35[b]	14.23	3.33×10^{-4}	14.23	7.89[e]	2.87	2.56	0.308
2.46[b]	11.36	3.43×10^{-4}	11.36	7.94[g]	2.65	2.3	0.252
4.04[c]	0.54	6×10^{-4}	0.54	8.30[f]	6	5.72	0.274
4.34[c]	0.375	8.77×10^{-4}	0.374	8.62[g]	11.28	11.03	0.253
4.64[c]	0.278	1.29×10^{-3}	0.277	8.91[g]	22.4	22.14	0.254
4.96[c]	0.26	2.46×10^{-3}	0.26	9.10[g]	32.4	32.2	0.244

[a] At zero buffer concentration; μ = 0.20 M; t = 20 °C. [b] HCl solutions (4.5×10^{-3}–6.5×10^{-2} M). [c] Acetate buffer. [d] Phosphate buffer. [e] *p*-Cyanophenoxide buffer. [f] Bicarbonate buffer. [g] Borate buffer.

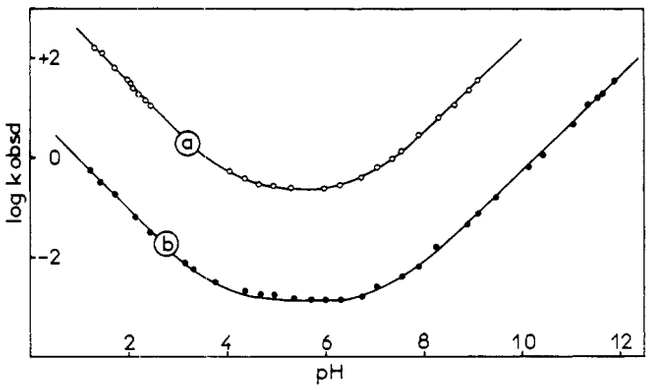

Figure 1. pH dependence of k_{obsd} (s^{-1}) for the formation and decomposition of adducts 5 (plot a) and 8 (plot b) in water: 20 °C, μ = 0.20 M.

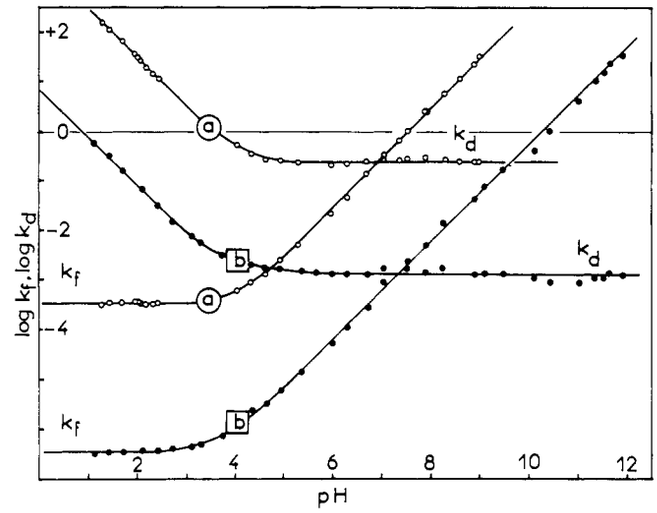

Figure 2. pH dependence of k_f (s^{-1}) and k_d (s^{-1}) for the formation and decomposition of adducts 5 (plots a) and 8 (plots b) in water: 20 °C, μ = 0.20 M.

glycol, gives a straight line of slope +1 in both cases and affords

$$K_a(5) = 1.38 \times 10^{-7}\ M^{+1}; \qquad K_a(8) = 5.5 \times 10^{-8}\ M^{+1}$$

Using eq 7, we also obtain values of K_c

$$K_c(5) = 1.17 \times 10^{7}\ M^{-1}; \qquad K_c(8) = 4.68 \times 10^{6}\ M^{-1}$$

Kinetic Measurements. The kinetics of the interconversion of **3, 6** and adducts **5, 8** were studied spectrophotometrically at 330 and 339 nm, respectively, by using stopped-flow as well as conventional methods. In all runs, the concentrations of acid, base, or buffer components were in large excess over substrate concentration, assuring pseudo-first-order kinetics throughout. The logarithmic values of the observed first-order rate constant k_{obsd} for the combined formation and decomposition of **5** and **8** at 20 °C are plotted in Figure 1 as a function of pH. Since buffer catalysis of the decomposition of **5** and **8** has been observed in the more acidic buffers (chloracetate, formate, and acetate buffers) the k_{obsd} values used at pH <5 in these pH profiles are those extrapolated to zero buffer concentration. In contrast, no buffer catalysis has been detected in the more basic buffers. As can be seen smooth pH–rate profiles were obtained despite the fact that buffers of varying chemical types were used.

The rate constant k_{obsd} reflects the rate of approach to equilibrium between the parent ethers and the adducts and can be expressed as the sum of the individual pseudo-first-order rate constants k_f and k_d, respectively, for the formation and decomposition of **5** and **8**. Using a treatment similar to one previously described[9,16] k_f and k_d may be calculated from eq 9 and 10 where $pH_{1/2}$ is the experimental pH value corresponding to the half-formation of **5** ($pH_{1/2}$ 6.98) and **8** ($pH_{1/2}$ 7.38).

$$k_f = \frac{k_{obsd}}{1 + (10^{-pH}/10^{-pH_{1/2}})} \tag{9}$$

$$k_d = \frac{k_{obsd}}{1 + (10^{-pH_{1/2}}/10^{-pH})} \tag{10}$$

Tables I and II present the values of k_f and k_d calculated in this way at 20 °C together with the experimental values of k_{obsd}.

Complete data are graphically represented in Figure 2 which shows the pH dependence of k_f and k_d. These pH profiles are consistent with equations of the form

$$k_f = k_1 + k_2K[OH^-] = k_1 + \frac{k_2KK_w}{a_{H^+}\gamma_\pm} \tag{11}$$

$$k_d = k_{-2} + k_{-1}[H^+] = k_{-2} + \frac{k_{-1}a_{H^+}}{\gamma_\pm} \tag{12}$$

Scheme I shows the reactions to which the various rate constants refer, viz., k_2 and k_1 refer to internal cyclization of the anions and the parent glycols, respectively, while k_{-2} and k_{-1} refer to the noncatalyzed and H^+-catalyzed ring opening of the adducts, respectively. The various rate coefficients could easily be determined from the two linear portions of the k_f and k_d pH rate profiles (high and low pH regions of each) respectively. We thus obtain: $Kk_2 = 3.1 \times 10^6\ M^{-1}\ s^{-1}$, k_{-2} =

Table II. Experimental and Calculated Pseudo-First-Order Rate Constants, k_{obsd}, k_f, and k_d, for the Formation and Decomposition of the Furoxanic Adduct 8 in Water[a]

pH	k_{obsd}, s^{-1}	k_f, s^{-1}	k_d, s^{-1}	pH	k_{obsd}, s^{-1}	k_f, s^{-1}	k_d, s^{-1}
1.12[b]	0.568	3.12×10^{-7}	0.567	6.72[g]	1.59×10^{-3}	2.85×10^{-4}	1.3×10^{-3}
1.42[b]	0.305	3.34×10^{-7}	0.304	7.05[g]	2.64×10^{-3}	8.41×10^{-4}	1.79×10^{-3}
1.72[b]	0.155	3.39×10^{-7}	0.154	7.52[h]	4.29×10^{-3}	2.48×10^{-3}	1.80×10^{-3}
2.12[b]	6.62×10^{-2}	3.64×10^{-7}	6.61×10^{-2}	7.89[h]	6.34×10^{-3}	4.84×10^{-3}	1.51×10^{-3}
2.42[b]	3.1×10^{-2}	3.40×10^{-7}	3.09×10^{-2}	8.23[h]	1.59×10^{-2}	1.39×10^{-2}	1.96×10^{-3}
2.72[b]	1.6×10^{-2}	3.69×10^{-7}	1.59×10^{-2}	8.91[i]	4.38×10^{-2}	4.25×10^{-2}	1.25×10^{-3}
3.12[b]	7.8×10^{-3}	4.29×10^{-7}	7.79×10^{-3}	9.11[i]	7.48×10^{-2}	7.34×10^{-2}	1.36×10^{-3}
3.30[c]	5.65×10^{-3}	4.70×10^{-7}	5.64×10^{-3}	9.47[i]	0.164	0.162	1.32×10^{-3}
3.74[d]	3.11×10^{-3}	7.12×10^{-7}	3.11×10^{-3}	10.16[i]	0.8	0.8	1.33×10^{-3}
4.34[e]	2.15×10^{-3}	1.96×10^{-6}	2.14×10^{-3}	10.42[i]	1.45	1.45	1.32×10^{-3}
4.64[e]	1.75×10^{-3}	3.17×10^{-6}	1.74×10^{-3}	11.05[j]	6.4	6.4	1.36×10^{-3}
4.94[e]	1.75×10^{-3}	6.33×10^{-6}	1.74×10^{-3}	11.35[j]	10.68	10.67	1.14×10^{-3}
5.36[f]	1.48×10^{-3}	1.40×10^{-5}	1.46×10^{-3}	11.53[j]	19.5	19.5	1.38×10^{-3}
5.68[f]	1.42×10^{-3}	2.77×10^{-5}	1.39×10^{-3}	11.65[j]	26.81	26.80	1.44×10^{-3}
5.98[g]	1.36×10^{-3}	5.20×10^{-5}	1.30×10^{-3}	11.89[j]	35.33	35.32	1.09×10^{-3}
6.30[g]	1.39×10^{-3}	1.06×10^{-4}	1.28×10^{-3}				

[a] At zero buffer concentration; $\mu = 0.20$ M; $t = 20$ °C. [b] HCl solutions (10^{-3}–0.1 M). [c] Citrate buffer. [d] Formate buffer. [e] Acetate buffer. [f] Succinate buffer. [g] Phosphate buffer. [h] *p*-Cyanophenoxide buffer. [i] Borate buffer. [j] NaOH solutions (10^{-3}–7×10^{-3} M).

Table III. Kinetic and Equilibrium Data for Spiro Complex Formation in Water and Deuterium Oxide

		5[a]	8[a]	10	12
H_2O	KK_2, M^{-1}	1.17×10^{7}[b]	4.68×10^{6}[b]	1.8×10^{7}[e]	3×10^{4}[b,h]
		1.24×10^{7}[c]	4.10×10^{6}[c]	2.1×10^{7}[c,f]	3.9×10^{4}[c,h]
				1.6×10^{7}[c,g]	
	Kk_2, $M^{-1}\,s^{-1}$	3.1×10^{6}	5.5×10^{3}	6.3×10^{5}[f]	9×10^{4}[h]
	k_{-2}, s^{-1}	0.25	1.34×10^{-3}	0.03[f]	2.3[h]
	k_1, s^{-1}	3.4×10^{-4}	3.3×10^{-7}		
		4.1×10^{-4}[d]	2.95×10^{-7}[d]		
	k_{-1}, $M^{-1}\,s^{-1}$	2.7×10^{3}	5.9	2.2×10^{3}[h]	1.8×10^{4}[h]
D_2O	KK_2, M^{-1}	2.17×10^{7}[c]	6.8×10^{6}[c]		
	Kk_2, $M^{-1}\,s^{-1}$	4.35×10^{6}	7.5×10^{3}		
	k_{-2}, s^{-1}	0.20	1.1×10^{-3}		1.7[h]
	k_1, s^{-1}	1.43×10^{-4}[d]	1.1×10^{-7}[d]		
	k_{-1}, $M^{-1}\,s^{-1}$	4.13×10^{3}	9.3	3.3×10^{3}[h]	
	KK_2 (H_2O)/KK_2 (D_2O)	0.57	0.60		
	Kk_2 (H_2O)/Kk_2 (D_2O)	0.71	0.73		
	k_{-2}(H_2O)/k_{-2} (D_2O)	1.25	1.22		1.35[h]
	k_1 (H_2O)/k_1 (D_2O)	2.86[i]	2.70[i]		
	k_{-1} (H_2O)/k_{-1} (D_2O)	0.65	0.63	0.66[h]	

[a] This work, $t = 20$ °C, $\mu = 0.2$ M. [b] KK_2 determined spectrophotometrically. [c] KK_2 calculated from the ratio Kk_2/k_{-2}. [d] k_1 calculated from $k_{-1} \times KK_2 \times K_w$ (D_2O)/$\gamma_\pm^2$ with pK_w (D_2O) = 15.05 at 20 °C. [e] Reference 18 at 25 °C. [f] Calculated at 20 °C from ref 17. [g] Reference 17 at 25 °C. [h] Reference 13b at 25 °C. [i] Calculated from the values of k_1 estimated according to footnote *d*.

0.25 s^{-1}, $k_1 = 3.4 \times 10^{-4}$ s^{-1}, and $k_{-1} = 2.7 \times 10^{3}$ $M^{-1}\,s^{-1}$ for **5** and $Kk_2 = 5.5 \times 10^{3}$ $M^{-1}\,s^{-1}$, $k_{-2} = 1.34 \times 10^{-3}$ s^{-1}, $k_1 = 3.3 \times 10^{-7}$ s^{-1}, and $k_1 = 5.9$ $M^{-1}\,s^{-1}$ for **8**. In both cases, the KK_2 values calculated from the ratio Kk_2/k_{-2} are in fairly good agreement with the KK_2 values determined spectrophotometrically (see Table III).

Inserting the values obtained for these parameters into the expression given by eq 13 for k_{obsd}, we see that at low pH (pH <4), only the reverse reaction of **5** (or **8**) + H^+ → **3** (or **6**) is important while, above pH 8, only the reaction of **3** (or **6**) + OH^- ⇌ **4** (or **7**) → **5** (or **8**) is important. This is in agreement with our experimental results.

$$k_{obsd} = \frac{k_{-1}a_{H^+}}{\gamma_\pm} + k_{-2} + k_1 + \frac{k_2 K K_w}{a_{H^+}\gamma_\pm} \qquad (13)$$

In the intermediate pH range, values of k_{obsd} are identical to those of k_{-2}, showing that the plateaus observed in the experimental pH profiles of Figure 1 correspond to the uncatalyzed ring opening of **5** and **8** and that adduct formation from internal cyclization of the glycols is negligible under our experimental conditions. Therefore, the intersections in Figure 1 between the k_{-2} plateaus and the straight lines of slope +1 yield the $pH_{1/2}$ values corresponding to the half-formation of **5** and **8**. We thus obtain $pH_{1/2}$ 6.93 and 7.36 for **5** and **8**, respectively, in excellent agreement with values determined thermodynamically.

As previously noted, buffer catalysis was observed in solutions of the most acidic buffers and was investigated in some detail with the chloracetate–chloracetic acid, formate–formic acid, and acetate–acetic acid systems. As is apparent from Figure 3 which presents the data for complex **8** in the acetate–acetic acid buffer, plots of the observed rate constant k_{obsd} vs. the undissociated acid concentration [AH] are linear with pH dependent intercepts but pH independent slopes. Thus, k_{obsd} can be expressed by eq 14 where k_{AH} is the second-order rate constant for catalysis of the ring opening of **5** and **8** by the buffer species AH:

$$k_{obsd} = k_{-2} + k_{-1}[H^+] + k_{AH}[AH] \qquad (14)$$

Table IV summarizes the k_{AH} values determined from the slopes for the three buffer systems. Also, as expected and shown in Figure 4, a plot of the intercepts vs. the hydrogen ion concentration affords in both cases a straight line with an intercept equal to k_{-2} and a slope equal to k_{-1}. We thus ob-

Table IV. Rate Constants k_{AH} for Acid Catalysis of the Ring Opening of Spiro Complexes in Water

buffer acidic species	pK_a[a]	k_{AH}, M^{-1} s^{-1}			
		5[b]	8[b]	10[c]	12[c]
H_3O^+	−1.74	2700	5.9	2200	18000
chloracetic acid	2.84	41	0.11	12	300
formic acid	3.74	11.7	0.024	2.3	60
acetic acid	4.64	4.75	0.011	0.9	25
water	15.66	7.2×10^{-5}	2.35×10^{-7}	2.14×10^{-6}	2.5×10^{-4}

[a] pK_a at μ = 0.20 M. [b] This work at t = 20 °C, μ = 0.20 M. [c] Reference 13b at t = 25 °C, μ = 0.30 M.

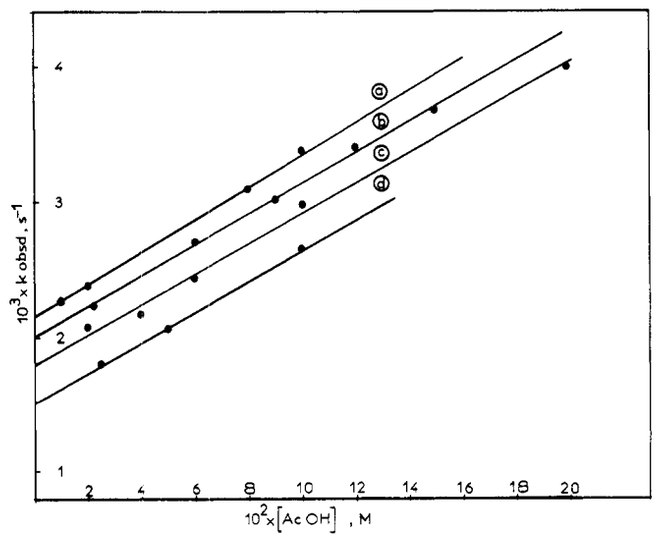

Figure 3. Effect of acetic acid concentration and pH on k_{obsd} for the decomposition of 8 in water: 20 °C, μ = 0.20 M; (a) pH 4.04; (b) pH 4.17; (c) pH 4.34; (d) pH 4.64.

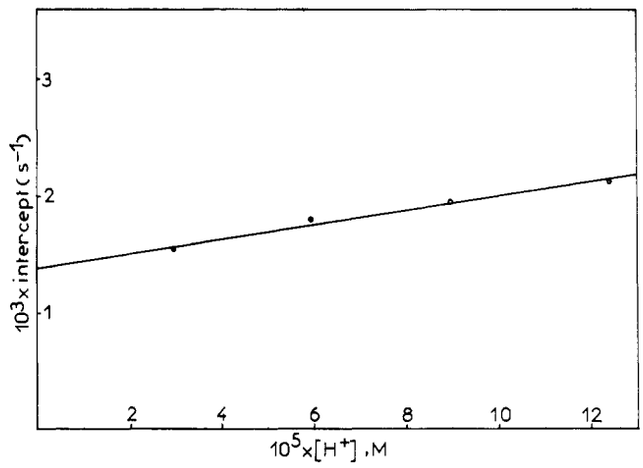

Figure 4. Plots of the intercepts of lines in Figure 3 against the hydrogen ion concentration: 20 °C; μ = 0.20 M.

tain: $k_{-2} = 1.38 \times 10^{-3}$ s^{-1}, $k_{-1} = 6.2$ M^{-1} s^{-1} for the benzofuroxan adduct 8 and $k_{-2} = 0.22$ s^{-1}, $k_{-1} = 2.5 \times 10^3$ M^{-1} s^{-1} for the benzofurazan adduct 5. Within experimental error, these values agree well with the one previously determined from the pH profiles of Figure 2.

The rates of formation and decomposition of 5 and 8 have also been determined in deuterium oxide at 20 °C. The observed solvent isotope effects on KK_2, Kk_2, k_{-2}, and k_{-1} are given in Table III.

Discussion

Effect of the Annelated Furazan and Furoxan Rings on Spiro Complex Formation. The values of equilibrium and rate constants for the formation and decomposition in water of spiro complexes 5 and 8 are collected in Table III which also includes some literature data on previously studied benzenic spirocomplexes 10 and 12 derived from 1-(2-hydroxyethoxy)-2,4,6-trinitrobenzene (9)[13b,17,18] and 1-(2-hydroxyethoxy)-2,4-dinitrophtalene (11).[13b] As can be seen from a comparison of the KK_2 values, the stability of the adducts 5 and 8 relative to the parent ethers is of the same order of magnitude as that of the trinitro adduct 10 (the ratios KK_2(10)/KK_2(5) and KK_2(10)/KK_2(8) are equal to 1.7 and 4.6, respectively) but much greater than that of the naphtalenic adduct 12 (the ratios KK_2(5)/KK_2(12) and KK_2(8)/KK_2(12) are equal to about 300 and 115, respectively). These results clearly demonstrate the very strong stabilizing influence exerted by the annelated furazan and furoxan rings on Meisenheimer-type adducts. That KK_2 is about 2.7-fold greater for 5 than for 8 indicates that the furazan moiety is somewhat more efficient than the furoxan one in stabilizing the adducts. Interestingly, this stability difference between 5 and 8 is similar to the one we have found between the adducts 13 and 14 formed from methanol and methoxide ion

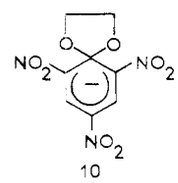
10

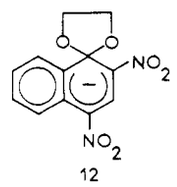
12

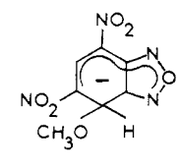
13

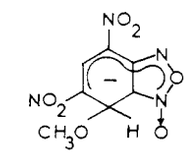
14

attack on 4,6-dinitrobenzofurazan and 4,6-dinitrobenzofuroxan in methanolic solution: pK_a(13) = 6.15;[19] pK_a(14) = 6.46.[20] These results are consistent with the notion that the electron-donating effect of the oxygen atom of the N-oxide group may partially reduce the overall electron-withdrawing effect of the furoxan ring compared with that of the furazan analogue.[21]

Despite their similar stability, 5 and 8 have drastically different rates of formation and decomposition. For the adduct formation, Kk_2 is about 560-fold greater for 5 than for 8, whereas the ratio k_1(5)/k_1(8) for direct internal cyclization of the parent ethers is found to be equal to about 1600. For adduct decomposition, the ratios k_{-2}(5)/k_{-2}(8) and k_{-1}(5)/k_{-1}(8) of the rate constants for the noncatalyzed and H^+-catalyzed ring opening are equal to about 200 and 700, respectively. One possible reason for differences in the rates of formation might be a stronger stabilization of the parent glycol 6 due to an intramolecular hydrogen bonding to the N-oxide group. This would decrease the equilibrium constant K governing the ionization of the side chain of 6, and hence Kk_2 for the formation of 8, as well as the k_1 value for direct internal cyclization of 6. However, this does not appear to be

an attractive explanation since such hydrogen bonding would require the formation of a nine-membered ring, a process which is not expected to be very favorable. There is evidence that it probably does not take place. If hydrogen bonding was present in **6**, one would expect different isotope effects on KK_2, Kk_2, and k_1 for **8** than on the similar terms for **5**. As can be seen in Table III, this is not borne out by the experimental data; in fact, the ratios $KK_2(H_2O)/KK_2(D_2O)$, $Kk_2(H_2O)/Kk_2(D_2O)$, and $k_1(H_2O)/k_1(D_2O)$ are about the same in the two systems. Also, we note that the values for the $KK_2(H_2O)/KK_2(D_2O)$ and $Kk_2(H_2O)/Kk_2(D_2O)$ ratios are identical to those recently reported by Bernasconi[17] for the formation of the spiro complex derived from 1-(3-hydroxypropoxy)-2,4,6-trinitrobenzene ($KK_2(H_2O)/KK_2(D_2O) = 0.585$; $Kk_2(H_2O)/Kk_2(D_2O) = 0.74$). Furthermore, there seems to be no compelling reason why a stronger stabilization of **6** should also affect the rate of decomposition of the adduct **8** relative to that of its analogue **5**. In fact, and in accord with previous discussions of similar situations,[22,23] any reasonable explanation of the slower rates of formation and decomposition of **8** must invoke an effect on the transition states which is not present (or present to a smaller extent) in either the reactants (**6** or **7**) or in the adduct **8**. We believe that this effect is connected with the presence of the *N*-oxide group and may be explained in terms of electrostatic considerations. Thus, we note that the negative glycolate oxygen can be removed from the N–O oxygen in the glycolate anion **7**, minimizing the repulsion, whereas in the adduct **8**, no negative charge is left on the glycolate oxygen. In contrast, important electrostatic repulsion between the two oxygens may be expected in the transition state **15**, which would result in an increase in its energy and in a concomitant decrease in the Kk_2 and k_{-2} values. When considering the k_1, k_{-1} pathway, similar electrostatic destabilization of the transition state **16** might arise

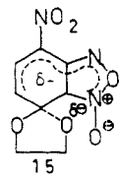

15

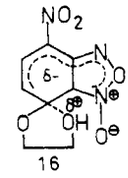

16

from repulsion between the partially positive glycolate oxygen and the positive aza nitrogen, causing a decrease in the k_1, k_{-1} values. Since similar effects cannot operate in furazan series, this would explain the higher rates of formation and decomposition for **5** than for **8**.

Buffer Catalysis. The present work shows the absence of buffer catalysis of the formation of the adducts **5** and **8**, indicating that, in the corresponding experimental conditions (pH >6), the parent ethers GOH and anions GO^- are in rapid equilibrium and the internal cyclization of these latter is rate determining. In contrast, under certain experimental conditions (pH <5), general acid catalysis of the decomposition of the adducts can be observed. As can be seen in Figure 5, plots of log k_{AH} values vs. the pK_a values for the catalyzing acids are linear with slopes giving values of 0.44 and 0.43, respectively, for the Brönsted coefficient α. These results are, indeed, quite similar to those reported by Crampton[13b] and Bernasconi[24] for the acid-catalyzed decomposition of benzenic spiro adducts **10**, **12**, **17**, and **18**. Also, as proposed by these authors,

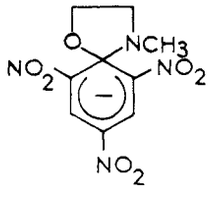

17

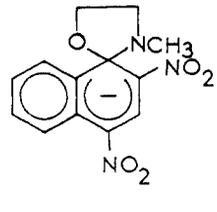

18

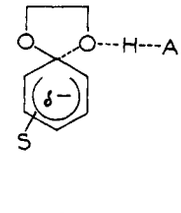

19

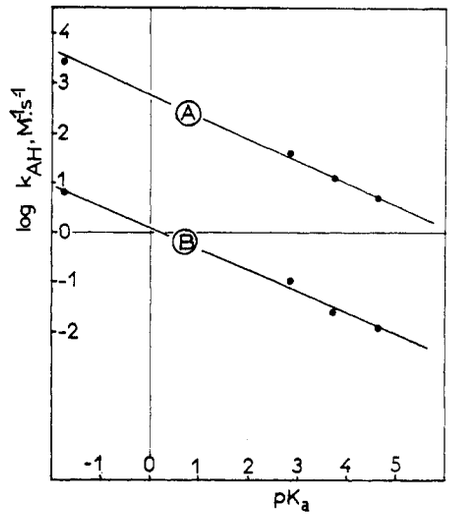

Figure 5. Brönsted plots for the acid catalyzed decomposition of adducts **5** (plot A) and **8** (plot B).

the most probable mechanism for the reaction is a concerted process, with a transition state such as **19**. The microscopic reverse of this step, i.e., general base-catalyzed cyclization of the ethers **3** and **6**, cannot be observed under conditions where buffer catalysis is effective because the equilibrium favors the ether over the complex, in agreement with the low values calculated for k_1.

An estimation, using the Brönsted plots of Figure 5, of the k_{AH} values for the less acidic general acids present in the buffer solutions ($H_2PO_4^-$, HCO_3^-, boric acid) confirms that the catalytic effects of these species are undetectable in our experimental conditions. Of special interest are the k'_{AH} values ($k_{AH} \times 55.55$) of 4×10^{-3} and 1.30×10^{-5} s^{-1} calculated for catalysis of the decomposition of **5** and **8**, respectively, assuming that water is acting as a general acid. Comparing the values with the experimental values of 0.25 and 1.21×10^{-3} s^{-1} measured for k_{-2} reveals, in agreement with the weak isotope effect found for this step ($k_{-2}(H_2O)/k_{-2}(D_2O)$ is of about 0.65 in both cases), that the noncatalyzed decomposition of the adducts does not occur via a biomolecular reaction involving the transition state **19** (A = OH) but is certainly a unimolecular reaction. Thus, the formation and decomposition of **5** and **8** are exclusively described by eq 2 at pH >5. At pH 5, the acid catalyzed ring opening of the adducts begins to compete with the noncatalyzed one and becomes the predominant pathway at pH <4.

Experimental Section

Materials. 7-(2-Hydroxyethoxy)-4-nitrobenzofurazan (**3**) and -benzofuroxan (**6**) were prepared at room temperature by adding 5 mL (5 *m*M) of 1 M sodium glycolate in ethylene glycol dropwise to a suspension of 1 g (≃5 mM) of 7-chloro-4-nitrobenzofurazan or -benzofuroxan in 40 mL of ethylene glycol. The solutions were allowed to stand for 1 h and then acidified by concentrated hydrochloric acid, diluted with water, and extracted with chloroform or ethyl acetate. After repeated washing with dilute hydrochloric acid solutions, the $CHCl_3$ or ethyl acetate solutions were dried over $MgSO_4$ and evaporated to yield brown crystals of **3** or **6** which were recrystallized from ethanol or a $CHCl_3$–acetone mixture: **3**, mp 115 °C; **6**, mp 124 °C.

The spiro adducts **5** and **8** were prepared as potassium salts by addition of nearly 1 equiv of 1 M methanolic potassium methoxide to a solution of the parent molecules **3** and **6** in acetonitrile. After the reaction, the solvent was evaporated off and the solid residues were washed repeatedly with anhydrous ether and then dried in vacuo. The adducts so obtained showed UV-visible and ^1H NMR spectra identical to those obtained when they were generated in situ from base addition to aqueous or Me_2SO solutions of the parent ethers. Acidification resulted in quantitative regeneration of the starting materials.

HCl and KOH solutions were prepared from Titrisol. Buffer solsolutions[9] were made up from the best available commercial grades of reagents.

Rate and pH Measurements. Stopped-flow determinations were performed on a Durrum stopped-flow spectrophotometer, the cell compartment of which was maintained at 20 ± 0.5 °C. Other kinetic measurements were made using a Beckman Acta-3 spectrophotometer. All kinetics runs were carried out under pseudo-first-order conditions with a substrate concentration of about 4×10^{-5} M. Rate constants are accurate to ±3%.

The pH was measured on a Radiometer Model pH meter according to standard methods. The pH values are relative to the standard state in pure water. The pD values were obtained by adding 0.40 to the pH meter reading.[25]

Acknowledgments. We are very thankful to Professor Claude F. Bernasconi (University of California—Santa Cruz) for helpful suggestions and assistance in the preparation of the manuscript.

Registry No.—**3**, 66770-00-1; **5** potassium salt, 66770-01-2; **6**, 66770-02-3; **8** potassium salt, 66787-92-6; 7-chloro-4-nitrobenzofurazan, 10199-89-0; 7-chloro-4-nitrobenzofuroxan, 18378-13-7.

References and Notes

(1) (a) E.N.S.C.P.; (b) Faculté des Sciences de Rouen.
(2) P. B. Ghosh and M. W. Whitehouse, *J. Med. Chem.*, **11**, 305 (1968).
(3) M. W. Whitehouse and P. B. Ghosh, *Biochem. Pharmacol.*, **17**, 158 (1968).
(4) P. B. Ghosh, B. Ternai, and M. W. Whitehouse, *J. Med. Chem.*, **15**, 255 (1972).
(5) W. P. Norris and J. Osmundsen, *J. Org. Chem.*, **30**, 2407 (1965).
(6) A. J. Boulton and D. P. Clifford, *J. Chem. Soc.*, 5414 (1965).
(7) (a) L. Di Nunno, S. Florio, and P. E. Todesco, *J. Chem. Soc., Perkin Trans. 2*, 1469 (1975); (b) D. Dal Monte, E. Sandri, L. Di Nunno, S. Florio, and P. E. Todesco, *Chim. Ind. (Milan)*, **53**, 940 (1971).
(8) (a) F. Terrier, F. Millot, and W. P. Norris, *Bull. Soc. Chim. Fr.*, 551, (1975); (b) F. Terrier, F. Millot, A. P. Chatrousse, M. J. Pouet, and M. P. Simonnin, *Org. Magn. Reson.*, **8**, 56 (1976).
(9) F. Terrier, F. Millot, and W. P. Norris, *J. Am. Chem. Soc.*, **98**, 5883 (1976).
(10) (a) E. Buncel, N. Chuaqui-Offermanns, and A. R. Norris, *J. Chem. Soc., Perkin Trans. 1*, 415 (1977); (b) E. Buncel, N. Chuaqui-Offermanns, B. K. Hunter, and A. R. Norris, *Can. J. Chem.*, **55**, 2852 (1977).
(11) A. P. Chatrousse and F. Terrier, *C. R. Hebd. Seances Acad. Sci., Ser. C*, **232**, 195 (1976).
(12) (a) C. F. Bernasconi and C. L. Gehriger, *J. Am. Chem. Soc.*, **96**, 1092 (1974); (b) C. F. Bernasconi and F. Terrier, *J. Am. Chem. Soc.*, **97**, 7458 (1975); (c) C. F. Bernasconi and R. H. De Rossi, *J. Org. Chem.*, **38**, 500 (1973); (d) C. F. Bernasconi and H. S. Cross, *ibid.*, **39**, 1054 (1974); (e) C. F. Bernasconi, C. L. Gehriger, and R. H. De Rossi *J. Am. Chem. Soc.*, **98**, 8451 (1976).
(13) (a) M. R. Crampton, *J. Chem. Soc., Perkin Trans. 2*, 2157 (1973); (b) M. R. Crampton and M. J. Willison, *ibid.*, 1681, 1686 (1974); (c) *ibid.*, 901 (1976).
(14) E. J. Fendler, J. H. Fendler, W. E. Byrne, and C. E. Griffin, *J. Org. Chem.*, **33**, 4141 (1968).
(15) H. S. Harned and W. J. Hamer, *J. Am. Chem. Soc.*, **55**, 2194 (1933).
(16) F. Terrier, F. Millot, and J. Morel, *J. Org. Chem.*, **41**, 3892 (1976).
(17) C. F. Bernasconi and J. R. Gandler, *J. Org. Chem.* **42**, 3387 (1977).
(18) J. Murto, *Suom. Kemistil. B*, **38**, 255 (1965).
(19) F. Terrier and A. P. Chatrousse, unpublished results.
(20). F. Terrier, A. P. Chatrousse, C. Paulmier, and R. Schaal, *J. Org. Chem.*, **40**, 2911 (1975).
(21) R. K. Harris, A. R. Katritzky, S. Øksne, A. S. Bailey, and W. G. Paterson *J. Chem. Soc.*, 197 (1963).
(22) C. F. Bernasconi and R. G. Bergstrom, *J. Am. Chem. Soc.*, **95**, 3603 (1973).
(23) A. J. Kresge, *Chem. Soc. Rev.*, **2**, 475 (1973).
(24) C. F. Bernasconi, C. L/ Gehriger, and R. H. De Rossi, *J. Am. Chem. Soc.*, **98**, 8451 (1976).
(25) P. K. Glascoe and F. A. Long, *J. Phys. Chem.*, **64**, 188 (1960).

Reversed Micellar Catalysis. Catalysis of Dodecylammonium Propionate Reversed Micelles in the Hydrolysis of Alkyl *p*-Nitrophenyl Carbonates

Hiroki Kondo, Kenjiro Fujiki, and Junzo Sunamoto*

Department of Industrial Chemistry, Faculty of Engineering, Nagasaki University, Nagasaki 852, Japan

Received December 20, 1977

The hydrolysis rates of methyl and dodecyl *p*-nitrophenyl carbonates in nonpolar organic solvents such as benzene and hexane were greatly enhanced by dodecylammonium propionate, DAP. The rate of hydrolysis was proportional to the square of the detergent concentration. At higher concentration of water than about 1×10^{-1} M the rate decreased with the increase in water concentration, while at lower concentration than 1×10^{-1} M the rate was almost irrespective of the water content. The rate varied greatly among five nonpolar solvents adopted, which was interpreted in terms of the substrate partitioning into the micellar core. Thermodynamic parameters of activation suggest that the mobility of the activation complex is highly restricted at the transition state ($\Delta S^{\ddagger} = -30$ to -53 eu), nevertheless the large rate enhancement is brought about by the term of enthalpy of activation ($\Delta H^{\ddagger} = 2$–11 kcal mol^{-1}), which overwhelms the unfavorable enthropy term. Hexadecyltrimethylammonium propionate was about fourfold less effective to the reaction than DAP, while benzyldimethylhexadecylammonium chloride showed no catalytic effect at all under the same reaction conditions.

Reversed micellar catalysis is roughly classified into two categories: (1) the catalysis by detergent itself in the reversed micelles provided with the functional detergents and (2) the assistance of the restricted (rigid) field produced in the interior core of reversed micelles. The former is exemplified in studies such as the mutarotation of glucose,[3] the decomposition of Meisenheimer complex,[4] and the hydrolyses of sucrose,[5] ATP,[6] and 2,4-dinitrophenyl sulfate,[7] where the general acid–base catalysis with detergents is concerned. The latter cases are seen in the ATP hydrolysis as catalyzed with the Mg^{2+} ion[6] and the aquation of tris(oxalato)chromate(III).[8]

In this work, through the kinetic investigation for the hydrolytic decomposition of alkyl *p*-nitrophenyl carbonates in the DAP reversed micelles, which belongs to the category (1), we would like to extend the scope of reversed micellar catalysis.

Experimental Section

Materials. Dodecylammonium propionate (DAP) was prepared according to the method described earlier.[9] Hexadecyltrimethylammonium propionate (CTAP) was prepared by the replacement of the counteranion of hexadecyltrimethylammonium hydroxide with propionic acid by the aid of the anion exchange column chromatography (Amberlite IRA-400) technique. The surfactant, CTAP, was very hygroscopic and difficult to submit to the elemental analysis. CTAP was stored over phosphorus pentaoxide in a vacuum desiccator and the purity was established by TLC, IR, and NMR spectra. Benzyldimethylhexadecylammonium chloride (CBDACl) was commercially obtained. Syntheses of methyl- (**1a**) and dodecyl-*p*-nitrophenyl carbonates (**1b**) are described elsewhere.[10] Distilled water using a glass distillator was used throughout all the kinetic runs. All the organic

0022-3263/78/1943-3584$01.00/0